

Development of a digital mammography system

M.J. Yaffe, R.M. Nishikawa, A.D.A. Maidment and A. Fenster*

Departments of Medical Biophysics and Radiology
University of Toronto and Physics Division, Ontario Cancer Institute
500 Sherbourne Street, Toronto, Ontario, Canada M4X 1K9

* Imaging Research Laboratories, John P. Robarts Research Institute
100 Perth Drive, London, Ontario, Canada N6A 5K8

ABSTRACT

A digital breast imaging system is under development to provide improved detectability of breast cancer. In previous work, the limitations of screen-film mammography were studied using both theoretical and experimental techniques. Important limitations were found in both the acquisition and the display components of imaging. These have been addressed in the design of a scanned-projection digital mammography system. A high resolution x-ray image intensifier (XRII), optically coupled to a self-scanned linear photodiode array, is used to record the image. Pre- and post-patient collimation virtually eliminates scattered radiation and veiling glare of the XRII with only a 20% increase in dose due to penumbra. Geometric magnification of 1.6 times is employed to achieve limiting spatial resolution of 7 lp/mm. For low-contrast objects as small as 0.1 mm in diameter, the digital system is capable of producing images with higher contrast and signal-to-noise ratio than optimally-exposed conventional film-screen mammography systems. Greater latitude is obtainable on the digital system because of its wide dynamic range and linearity. The slit system is limited due to long image acquisition times, and poor quantum efficiency. This motivated our current work on a slot beam digital mammography system which is based on a fiber-optic x-ray detector. Preliminary results of this system will be presented.

1. INTRODUCTION

Breast cancer is one of the major cancer killers of women, affecting about one in 11 North American women¹. There is evidence that, for women 50 to 59 years of age, the mortality from breast cancer can be reduced with early detection², and there are indications that this benefit may extend to women in the 40 to 49 year age group³. Mammography is the most sensitive technique currently available for the detection of minimal breast cancer^{4,5}, and film-screen imaging is the most common mammographic technique in use today. While the quality of film-screen mammographic images has increased tremendously in the last 15 years, several fundamental limitations exist.

2. LIMITATIONS OF FILM-SCREEN MAMMOGRAPHY SYSTEMS

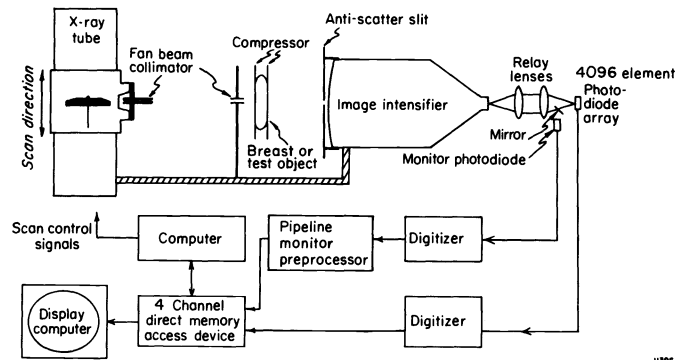
High-quality mammography requires images which exhibit both excellent spatial resolution and contrast sensitivity. In previous work^{6,7} we analysed the performance of several state-of-the-art film-screen mammography systems and determined that they are limited in their performance for displaying structures of low contrast typical of mammary tumours and microcalcifications. This limitation is a result of the restricted dynamic range over which radiographic film provides significant display contrast. As well, film granularity reduces the image signal-to-noise ratio (SNR), especially at higher spatial frequencies. A further problem is related to the use of a broad area image receptor, since even at the low energies used for mammography, the resulting scatter-to-primary (S/P) ratio is significant. The reduction of S/P by a factor of 3 (using a conventional mammography grid) requires approximately twice the radiation dose to the patient.

3. DIGITAL SLIT-BEAM MAMMOGRAPHY

We have developed a prototype scanned-projection digital mammography (SPDM) system⁷ to overcome the limitations of film-screen mammography. The processes of image acquisition and display have been separated so that each process can be optimized independently. The system, shown in Figure 1, employs a high resolution x-ray image intensifier (XRII) optically coupled to a Reticon self-scanning linear photodiode array containing 1024 elements. In this system, an x-ray beam confined to a thin slice irradiates the breast with the transmitted quanta entering the XRII via a narrow slit placed across its diameter. The intensified and minified image from the XRII is projected onto the photodiode array by a pair of relay lenses. Each element of the diode array is 25 μ m in width and 2.5 mm in length. The video output of the diode array is digitized to 16-bit accuracy and transferred to a computer. A two-dimensional image is obtained by scanning the breast with the fan-beam of x rays.

The SPDM system employs a 45 kVp tungsten spectrum filtered by 0.4 mm of aluminum, with a capacitor smoothed, three-phase waveform. Geometric magnification of 1.6 (with a 0.2 mm focal spot) is employed to increase the spatial resolution of the system. The source-detector distance is 60 cm. The post-patient slit is 0.127 mm in width, and the pre-patient slit is 0.080 mm in width. With the current choice of

Figure 1. Schematic representation of the scanned-projection digital mammography system. The image intensifier has an input diameter of 17 cm and an output diameter of 25 mm.



lenses, measurements from 3 adjacent diode elements are averaged to obtain square pixels corresponding to about 0.080 mm by 0.080 mm in the patient entrance plane. Recently, the field of view has been increased by replacing the diode array with one containing 4096 elements of dimension 15 μm by 508 μm .

An independent monitor channel measures the light produced by the image intensifier in a region of its field of view that is exposed to the unattenuated x-ray beam. This addresses the problem of artifacts caused by the fluctuation of the x-ray source, and the XRII gain. The monitor signal can then be used to correct image signal measurements from the photodiode array. The correction process is complicated by the readout cycle of the diode array, in that each array element measures the radiation signal over a slightly different time period. To solve this problem, we designed a dedicated "pipeline" processing circuit that analyzes the monitor data, calculates the proper correction value, and applies the correction to the measurement from each photodiode element. With the correction circuit, we have demonstrated that the effects of systematic x-ray fluence variations can be reduced by an order of magnitude to a level that is lower than quantum noise.

The fixed pattern noise (FPN) of the XRII is a large component of the total noise. The FPN can be attributed to imperfections and nonuniformities in the output phosphor, the input phosphor, the photocathode, and the glass vacuum bottle. In addition, the glass vacuum bottle has been coated with black paint and a translucent protective plastic, both of which are spatially nonuniform. The relatively low x-ray energies used cause these sources of structural mottle to be of importance. Fortunately, this structure is temporally invariant and can be subtracted from the image. A correction process is used to eliminate significant diode-to-diode sensitivity variations in the Reticon.

With the corrections described above, the limiting spatial resolution of our system (measured with a high contrast Funk bar pattern) is about 7.2 lp/mm, while the limiting resolution of state-of-the-art film-screen mammography exceeds 16 lp/mm. Limiting resolution describes the performance of detecting high contrast objects and is not indicative of the detection of low contrast objects, as required for structures in mammography. Contrast-detail analysis is a more appropriate characterization. The results of such a test are illustrated in Figure 2, where the contrast-detail measurements of a state-of-the-art film-screen mammography system and our current SPDM system are compared. It is clear that SPDM is capable of detecting structures of lower contrast than the film-screen system. With SPDM, detection was improved by at least a factor of 2 for any diameter object, in spite of the inferior limiting resolution of SPDM. Intuitively, one would expect that the curves would cross; the film-screen system being superior for small objects due to its higher spatial resolution. The curves fail to cross due to the SNR of the film, which falls off at higher spatial frequencies due to granularity.

The contrast-detail curves of Figure 2 were obtained with optimal exposure to the film-screen system; i.e., such that the maximum SNR was obtained. On any realistic image, low frequency variations in anatomical structure would cause parts of the image to be exposed in a region of the characteristic curve of the film that provided suboptimal SNR. This is illustrated in Figure 3 where the SNR of the film-screen system (Kodak OM-1 with Min-R screen) is plotted as a function of exposure to the screen. This calculation is based on data of Bunch *et al.*⁸ Also shown is the SNR of the SPDM system, which is affected primarily by quantum noise, and therefore, monotonically improves with exposure.

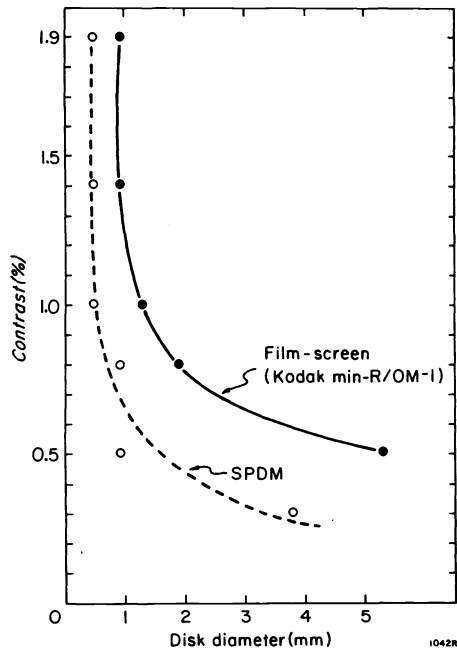


Figure 2. Contrast-detail measurements of a film-screen mammography system and our SPDM system for equivalent mean-glandular doses to the breast phantom.

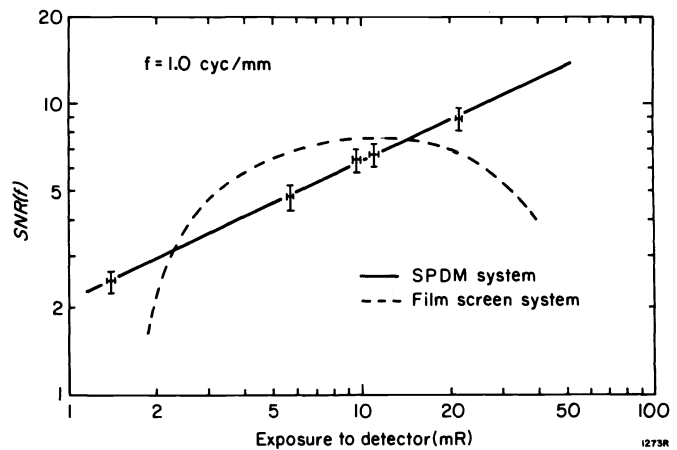


Figure 3. SNR at 1 cycle/mm as a function of detector exposure for a film-screen mammography system and our SPDM system.

4. LIMITATIONS OF SLIT-BEAM MAMMOGRAPHY

We have used our SPDM system to produce high quality images with sufficient spatial resolution and contrast sensitivity for diagnostic mammography. However, it is limited by several intrinsic characteristics of sequential single-line acquisition and the use of an XRII as the detector. There are four specific areas of concern: 1) imaging time; 2) x-ray tube heat loading; 3) XRII detective quantum efficiency (DQE) and geometry; and, 4) increase in dose due to penumbra.

The most important limitation is the image acquisition time, which for a 2048 line image is currently several minutes. Imaging time is dependent on the required quantum statistics, the exposure rate of the x-ray tube, and the number of lines contained in the image. Sequential single-line acquisition makes very inefficient use of x-ray tube heat loading, since only 0.01% of the x-ray tube output is actually used to create the image.

The use of an XRII presents several problems. The XRII is costly, bulky, and difficult to incorporate into the geometry of a mammography system. The image field of a mammogram is rectangular; the long dimension being across the chest of the patient. The circular format of the XRII requires that the scan direction be in this long dimension, thus requiring more scan lines to be measured. In addition, only a small fraction (0.05%) of the input surface of the XRII is actually used to produce an image. Finally, the input phosphor of the XRII is inside the vacuum window, and was not designed for imaging at potentials of 45 kVp and lower, as used in our system. Attenuation by the window reduces the quantum efficiency to only about 25%.

The final problem associated with an SPDM system is the increase in dose due to penumbra. In our system with a 0.080 mm slit width at the patient and geometric magnification of 1.6, a 20% increase in dose occurs due to penumbra. This is offset by the dose efficiency of the scatter elimination achieved. The penumbra dose could be reduced if a smaller focal spot were used. Unfortunately, this decreases the maximum continuous heat loading of an x-ray tube.

In our prototype, we are implementing improvements to reduce scan time. We have acquired an x-ray tube which provides greater output, and a beryllium window XRII which will significantly improve the quantum efficiency of the system, thereby reducing either the exposure rate (and hence the x-ray tube loading) or the time required for a given exposure.

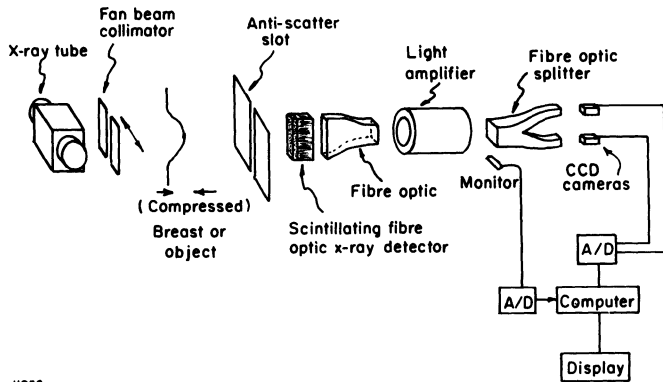


Figure 4. Schematic representation of the proposed scanned slot-beam digital mammography system. For simplicity one light amplifier and two CCD cameras are shown.

11958

5. SLOT-BEAM MAMMOGRAPHY

We are currently in the process of designing a slot-beam digital mammography system that addresses many of the problems presented above. The proposed system is illustrated in Figure 4. The pre-patient collimator restricts the x rays to a slot-beam which is incident upon the compressed breast. The transmitted quanta enter a matched post-patient slot which is between 2.5 and 5 mm in width. The slot defines the detector entrance aperture and allows the simultaneous acquisition of 50 to 100 image lines, thereby decreasing the required imaging time by that factor. The detector itself will be described below.

5.1. Scattered radiation

As the volume of breast that is simultaneously irradiated increases, the scattered radiation component in the beam reaching the detector will also increase. The effect of beam thickness on the scatter-to-primary ratio was measured in our laboratory for an x-ray beam of 30 kVp and a 6.0 cm thick BR12 breast phantom (typical of a thick breast), and is shown in Figure 5. For a slot size of 5 mm, S/P is approximately 0.06. Although this reduces the performance of the system from the slit geometry, where S/P is approximately 0.01, we believe that use of simple anti-scatter devices such as an "air-core" grid (currently under investigation) can reduce the S/P by a factor of 5 while necessitating an exposure increase of only about 10%. The width of the slot-beam in the final design will be chosen as a tradeoff between the decrease in imaging time due to concurrent multiple-line acquisition and the decrease in useful dynamic range of the detector caused by the increased scattered radiation.

5.2. Veiling glare

The adoption of the slot-beam geometry also imposes a compromise in terms of the veiling glare of the XRII. The effect of slot width on veiling glare was examined experimentally and is illustrated in Figure 6 in terms of the drop in MTF at 0.2 cycles per mm. For a 5 mm slot, the drop would be about 10%. Although this may be tolerable, the additional considerations of improving detective quantum efficiency and detector geometry motivate our development of a more specialized slot-beam detector.

5.3. Detector design

In our current experimental system, the detector consists of a phosphor strip bonded to a fiber-optic faceplate. The faceplate is optically coupled to a light amplifier by a set of fiber-optic tapers and splitters. The light amplifier is a 25 mm, second generation, three-stage device, incorporating a micro-channel plate. This avoids veiling glare effects. The output phosphor of the light amplifier is coupled by fiber-optic tapers and splitters to a group of CCD arrays. By placing the x-ray absorbing material of the detector outside of the vacuum vessel, it is possible to eliminate losses due to window absorption of x rays. As well, a type and thickness of phosphor material can be selected which is more appropriate to the mammographic imaging process. These factors will allow an improvement in the detective quantum efficiency over our SPDM system.

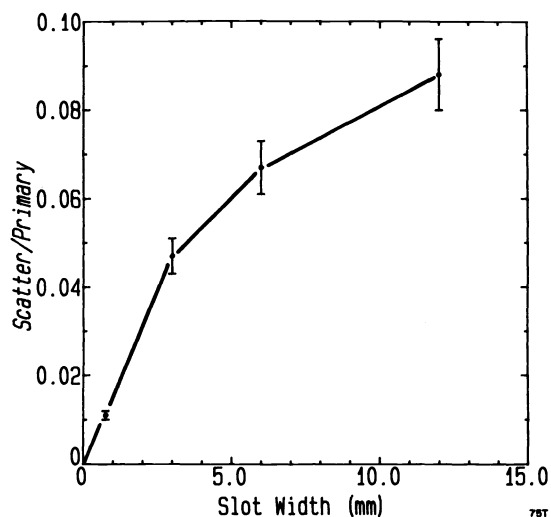


Figure 5. Increase of scatter-to-primary ratio as a function of slot width in mm.

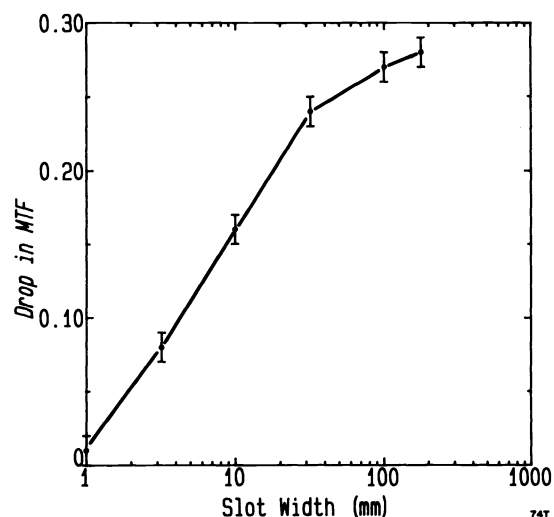


Figure 6. Drop in MTF, measured at 0.2 lp/mm, as a function of slot width in mm.

Another important feature of this detector design is that the geometry can be arranged to be much more appropriate for the scanning requirements of digital mammography. With a rectangular image field, it is preferable to scan in the shortest direction. Because the x-ray detection and amplification processes are separated in the slot-beam detector, it will be possible to produce a detector in a geometry allowing scanning in the short direction (i.e., from chestwall-to-nipple), thereby reducing image acquisition time. In the system currently under investigation, the active detection area will be 2.5 to 5 mm in width and 200 mm in length and will contain approximately 50 to 100 by 4096 discrete detector elements, each of dimension 50 μm . In initial work we are investigating use of a strip of gadolinium oxysulfide fluorescent screen (Min-R), optically coupled to a 1.0 numerical aperture fiber-optic faceplate. Details of the detector are provided in Figure 7. The 200,000 to 400,000 detector elements are coupled via fiber-optic bundles to one of m light amplifiers. Each of these in turn is optically coupled to n CCD arrays. The values of m and n will depend on the specifications of the device chosen for the final design: current values are $m = 2$, $n = 3$.

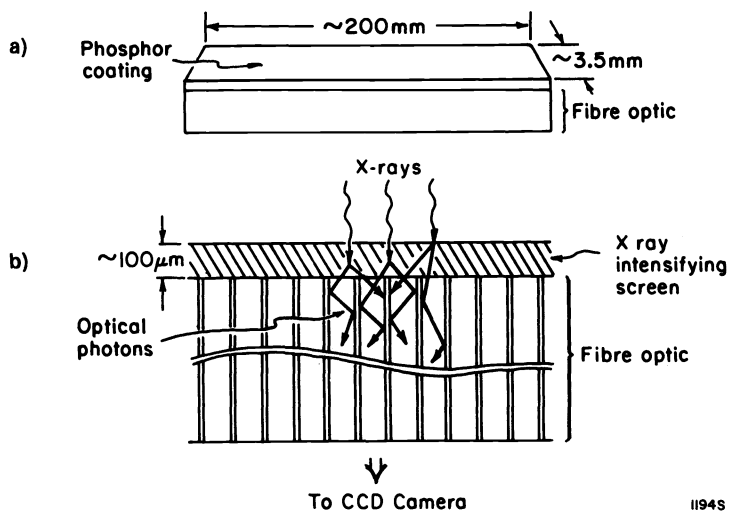


Figure 7. a) Schematic of the scintillating fiber optic x-ray detector; b) cross-sectional view.

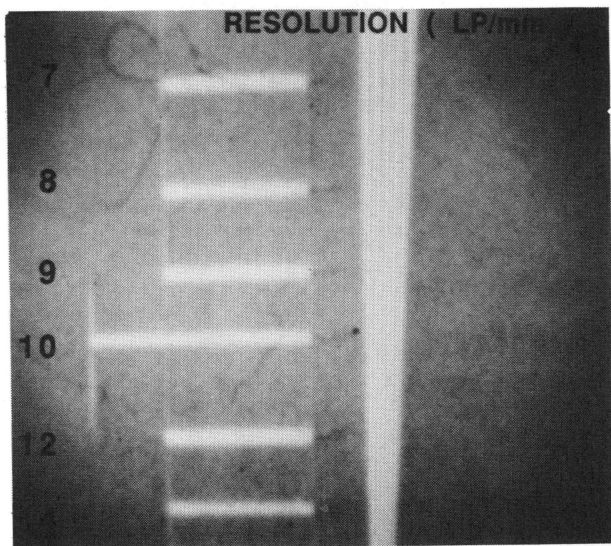


Figure 8. Digital image of a Funk star resolution pattern. Limiting resolution is about 12.5 lp/mm.

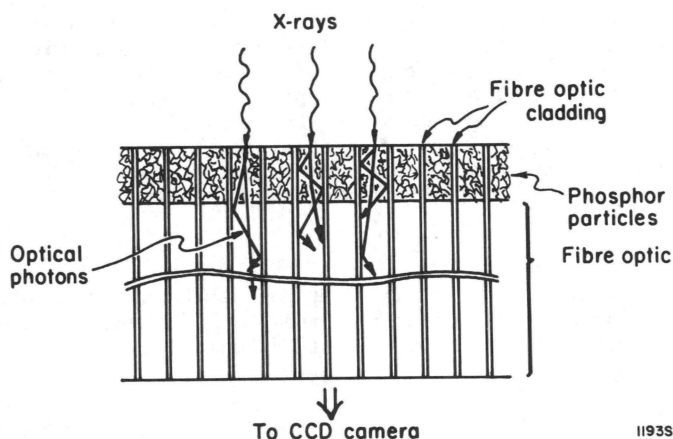


Figure 9. Intagliated fiber-optic detector (cross-sectional view).

5.4. Preliminary results

5.4.1 Limiting resolution

In initial experiments with this detector, limiting spatial resolution was measured using a Funk star resolution pattern. It is seen from Figure 8 that at this point a limiting resolution of approximately 12.5 lp/mm has been achieved. Additional experiments were conducted to determine the influence on resolution of the individual components in the imaging system. Since the light amplifier and optics provide limiting resolution of greater than 25 lp/mm, it appears that the system resolution is currently determined by the CCD, which at the present magnification has a limiting resolution of 15 lp/mm. This will be verified with MTF analysis, which is currently in progress.

5.4.2 Linearity

All components in the system will exhibit spatial variations in sensitivity resulting in fixed-pattern image noise. Correction is greatly simplified if the system is linear; i.e., each of the cascaded components is linear.

The linearity of the light amplifier was evaluated, using a constant intensity integrating light sphere, illuminated by green LEDs that were chosen to match the spectra of gadolinium oxysulfide closely. The incident light intensity was varied over a range of 10^4 using neutral density filters. Deviation from linearity was less than 3% over this range. At greater intensities the light amplifier approaches saturation, while performance below this range could not be evaluated due to the noise limitations of the test equipment.

Work on characterizing our CCD camera is ongoing. Janesick et al.⁹ have characterized a number of CCDs and have found that the dynamic range of frame-transfer devices suitable for this application exceed 2000.

5.5. Future work

At present our work is concentrated on detector optimization and only a small scale model has been constructed. An insufficient field of view is available for performance of proper contrast-detail analysis. This work will be the subject of a future presentation.

Although we are pleased with the initial performance of the detector, we feel that it still may be possible to improve the quantum efficiency by increasing the phosphor thickness. We are investigating the application of phosphor directly to the fiber faceplate by means of "intagliation"^{10,11,12} as illustrated in Figure 9. Extramural optical attenuation material would prevent light generated in one fiber-optic core from travelling through the cladding to adjacent cores, thereby preserving spatial resolution.

5.5.1. Image readout and digitization

The large number of detector elements in the slot beam makes the recording of image data a formidable problem. We plan to couple the detector plate, the light amplifiers and the CCD arrays using "scrambled" or incoherent fiber-optic bundles, to reduce cost and increase flexibility. This would result in adjacent elements of the detector mapping to non-adjacent CCD elements or even elements on different CCDs. An unscrambling operation would then be used to re-establish the correspondence of measured data values. This could be accomplished in an initial calibration operation where the rectangular detector was scanned with either a fine pencil beam of x rays, or a laser. A PROM lookup table could then be created and this would be used to correct incoming data during image acquisition.

6. SUMMARY

The development of an experimental digital mammographic imaging system has been described. A scanning slit system has demonstrated the potential advantages of digital mammography in terms of improved contrast detectability. Development of a scanned-slot system to improve image-acquisition time and detective quantum efficiency is now underway.

7. ACKNOWLEDGEMENTS

We are grateful for assistance and advice contributed by Gordon Mawdsley, Richard Gerson, Peter Munro, David Holdsworth, Curtis Caldwell, Jeff Byng, Carl Nauman and Normand Robert. The generosity of Thomson CGR (France) and Machlett Laboratories in providing equipment to further this project is much appreciated. Financial assistance was provided by The National Cancer Institute of Canada, The Medical Research Council of Canada and The Ontario Cancer Treatment and Research Foundation. The second author is supported by an Ontario Graduate Scholarship.

8. REFERENCES

1. 1986 Cancer Facts and Figures, American Cancer Society.
2. S. Shapiro, W. Venet, et al., "Ten- to Fourteen-Year Effect of Screening on Breast Cancer Mortality", JNCI 69(2), 349-355, (1982).
3. L. Tabir, et al., "Reduction in Mortality from Breast Cancer After Mass Screening with Mammography", Lancet 1985:1, 829-832, (April 13 1985).
4. T.G. Frazier, E.M. Copeland, H.S. Gallager, D.D. Paulus, and E.C. White, "Prognosis and Treatment in Minimal Breast Cancer", Am. J. Surg. 133(6), 697-701, (1977).
5. G.D. Dodd, "Present status of thermography, ultrasound and mammography in breast cancer detection", Cancer 39(6), 2796-2805, (1977).
6. R.M. Nishikawa, and M.J. Yaffe, "Signal-to-noise properties of mammography film-screen systems", Med. Phys. 12(1), 32-39, (1985).
7. R.M. Nishikawa, G.E. Mawdsley, A. Fenster, and M.J. Yaffe, "Scanned-projection digital mammography", Med. Phys. 14(5), 717-727, (1987).
8. P.C. Bunch, K.E. Huff, and R. Van Metter, "Sources of noise in high-resolution screen-film radiography", in Application of Optical Instrumentation in Medicine XIV, R.H. Schneider and S.J. Dwyer III, eds., Proc. SPIE 626, 64-75, (1986).
9. J.R. Janesick, T. Elliot, and S. Collins, "Scientific charge-coupled devices", Opt. Eng. 26(8), 692-714, (1987).
10. V. Duchenois, M. Fouassier, and C. Piaget, "High-Resolution Luminescent Screens for Image Intensifier Tubes", in Advances in Electronics and Electron Physics, Vol. 64B, 365-371, (1985).
11. D.E. Osten, "Fiber-optic coupled CID-MCP detectors for scientific applications", in Solid State Imaging Arrays, Proc. SPIE 570, 89-94, (1985).
12. J. de Groot, J. Holleman, and H. Wallinga, "X-ray image sensor based on an optical TDI-CCD imager", in Solid State Imagers and Their Applications, Proc. SPIE 591, 24-30, (1985).